Submitted to International Journal of Solids and Structures

Self-equilibrium and Super-stability of Truncated Regular Hexahedral and Octahedral Tensegrity Structures

J.Y. Zhang [a,*] M. Ohsaki [b] F. Tsuura [c]

[a] *Graduate School of Design and Architecture, Nagoya City University, Japan*

[b] *Dept. of Architecture and Architectural Engineering, Kyoto University, Japan*

[c] *Dept. of Architecture and Urban Design, Ristumeikan University; currently Watami Co., Ltd.*

Abstract

This paper presents conditions for self-equilibrium as well as super-stability of the truncated regular hexahedral and octahedral tensegrity structures. Their symmetry can be described by octahedral group in group representation theory, and furthermore, their force density matrix is analytically rewritten in the symmetry-adapted form. The condition for self-equilibrium, in terms of force densities, is found by satisfying the non-degeneracy condition for a tensegrity structure. The condition for super-stability, also in terms of force densities, is further presented by guaranteeing positive semi-definiteness of the force density matrix.

Key words: Tensegrity; Hexahedral symmetry; Octahedral symmetry; Self-equilibrium; Super-stability; Group representation theory; Block-diagonalization.

1. Introduction

Tensegrity refers to the structure composed of continous tension and discontinuous compression (Fuller, 1962). The concept of tensegrity was born in arts, and nowadays, it has been widely applied in many different disciplines (Zhang and Ohsaki, 2015). For the purpose of further understanding of the whole class of truncated regular hexahedral and octahedral tensegrity structures, we present analytical conditions for their self-equilibrium as well as super-stability.

A truncated regular polyhedral tensegrity structure is generated from a truncated regular polygon (Zhang *et al.*, 2012). The cables lie along the edges of a truncated polyhedron, which is made by symmetrically cutting off the vertices of the polyhedron; and the struts are the diagonals connecting the vertices of the truncated polyhedron. The cables can be

* Address: 2-1-10 Kita-chikusa, Nagoya 464-0083, Japan.
Tel: +81-52-721-5348, Fax: +81-52-721-3110
E-mail: zhang@sda.nagoya-cu.ac.jp

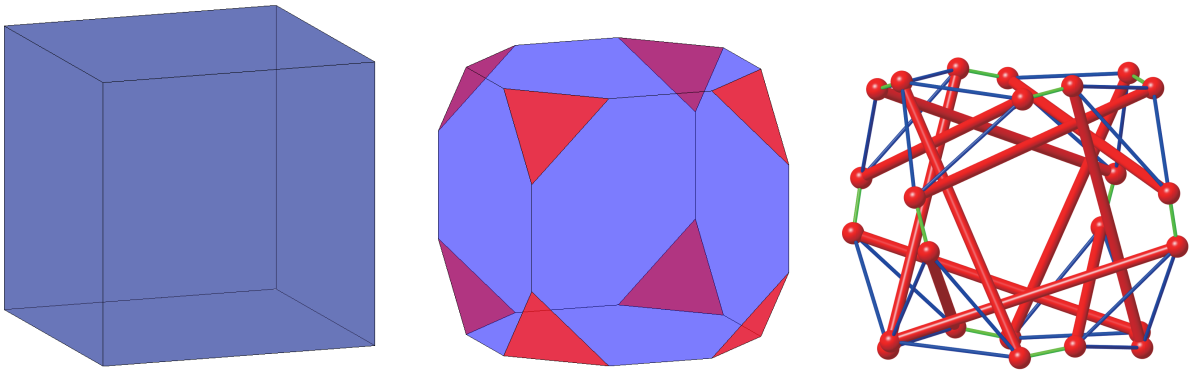

(a) regular hexahedron (b) truncated hexahedron (c) hexahedral tensegrity

Fig. 1. Generation of a truncated regular hexahedral tensegrity structure.

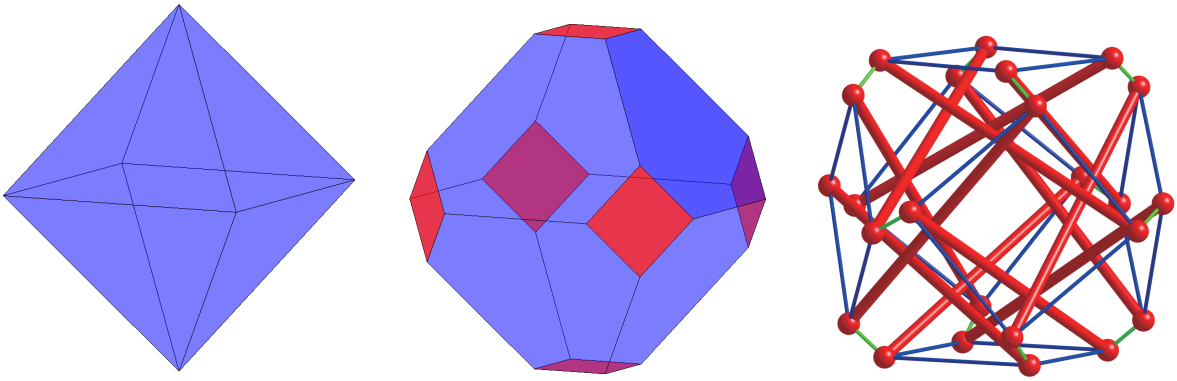

(a) regular octahedron (b) truncated octahedron (c) octahedral tensegrity

Fig. 2. Generation of a truncated regular octahedral tensegrity structure.

classified into two types: the *edge cables* lying on the original edges of the polyhedron, and the *cutting cables* lying on its cut edges.

Generation of the hexahedral and octahedral tensegrity structures studied in this paper is shown in Figs. 1 and 2, respectively. It is notable that a regular hexahedron and a regular octahedron are dual to each other, and both of them have the symmetry that can be described by octahedral group in group representation theory.

A truncated regular hexahedral or octahedral tensegrity structure consists of 24 nodes and 48 members, including 12 struts in compression and 36 cables in tension. Every node is connected by one strut, one edge cable, and two cutting cables. For both hexahedral and octahedral structures, there are 24 cutting cables and 12 edge cables.

According to the modified version of Maxwell's rule by Calladine (1978), the following relation holds:

$$\begin{aligned} n^{\mathrm{s}} - n^{\mathrm{m}} &= m - 3n + 6 \\ &= (12 + 36) - 3 \times 24 + 6 = -18, \end{aligned} \tag{1}$$

where n^{s}, n^{m}, m, and n respectively denote number of independent prestress modes, number of infinitesimal mechanisms, number of members, and number of nodes. It should be noted that the number of rigid-body motions, which is 6 for a three-dimensional structure,

is included in Eq. (1) because a tensegrity structure is free-standing, without any supports to constrain the rigid-body motions.

Both of the hexahedral and octahedral structures have only one mode of prestress; i.e., $n^{\mathrm{s}} = 1$, thus, there exists in total 19 infinitesimal mechanisms; i.e., $n^{\mathrm{m}} = 19$. It is this single prestress mode that stiffens the 19 infinitesimal mechanisms to make the structure stable, in the sense of having the minimum potential energy. The minus sign in Eq. (1) indicates that the structure is not *stable*, if no prestress is introduced. However, as will be proved later in this study, these structures can be *super-stable* if their members carry appropriate prestresses (or force densities).

Post-buckling behavior of the octahedral structure has been studied by Rimoli (2018); and it was further used as an elementary cell for a tensegrity-based planet lander (Rimoli and Pal, 2017). For further applications of these structures, it is necessary to thouroughly understand their (static) properties, including self-equilibrium and (super-)stability.

In our previous study (Tsuura *et al.*, 2010), the authors have numerically presented the conditions of self-equilibrium as well as super-stability for the tetrahedral, hexahedral, and octahedral structures. However, numerical approaches may miss the opportunity to have thorough understanding of self-equilibrium and stability properties of the structures, and hence, analytical results are always preferable as long as they are available. Zhang *et al.* (2012) presented a unified analytical solution for self-equilibrium of truncated regular polyhedral tensegrity structures, including the tetrahedral, hexahedral, octahedral, dodecahedral, and icosahedral structures. The conditions for super-stability of these structures, however, have been investigated in a numerical way.

In this study, we present the equilivalent self-equlibrium and super-stability conditions for the truncated regular hexahedral and octahedral structures in a rigorous way – with the least numerical computations. In our previous studies (Zhang *et al.*, 2009a, 2010; Zhang and Ohsaki, 2012), the authors have demonstrated the power of presenting analytical solutions for the structures with high-level of symmetry via group representation theory. In this study, we follow the same procedure as in our previous studies: (1) derive the symmetry-adapted form of the force density matrix, (2) find the condition for self-equilibrium by enforcing the force density matrix to have nullities of four, and (3) find the condition for super-stability so that the force density matrix is positive semi-definite.

It is notable that the conditions were derived based on symmetry of force densities, rather than symmetry of the structure. A tensegrity structure can have infinite possibilities of geometry realizations with the same set of force densities; different geometry realizations are related through affine motions (Zhang and Ohsaki, 2015). In other words, we can always have an asymmetric geometry realization of the truncated hexahedral or octahedral tensegrity structure, while its force densities have the hexahedral or octahedral symmetry.

Following this introductory section, the paper is organized as follows: Section 2 describes configuration and symmetry of the hexahedral and octahedral structures; Section 3 presents the analytical symmetry-adapted form of the force density matrix; Section 4 finds the self-equilibrium and super-stability conditions for the hexahedral structures, in terms of force densities; Section 5 finds the self-equilibrium and super-stability conditions for the octahedral structures; and Section 6 briefly concludes the study.

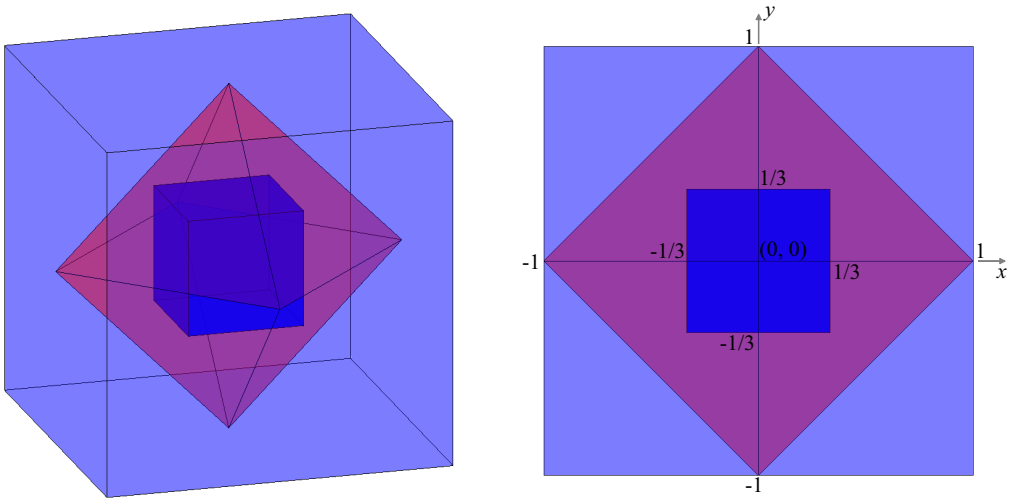

(a) top view (b) side view

Fig. 3. Duality of hexahedron and octahedron.

2. Hexahedral and Octahedral Symmetry

Symmetry of a structure can be systematically dealt with by using group representation theory. The symmetry-adapted form of the force density matrix is necessary for derivation of the self-equilibrium and super-stability conditions for the hexahedral and octahedral structures. Moreover, the symmetry-adapted force density matrix relies on irreducible representation matrices. Thus, this section gives a brief introduction to the octahedral group and its irreducible representation matrices. More general details about group representation theory can be found, for example, in the textbook by Bishop (1973) or Kettle (1995).

2.1 Duality of hexahedron and octahedron

A hexahedron (cube) has 8 points, 6 faces, and 12 edges. The adjacent edges are perpendicular to each other, forming 90 degree angles. An octahedron has 6 points, 8 faces, and 12 edges. Duability of a hexahedron and an octahedron can also be observed in Fig. 3:

- If the mid-points of adjacent faces of a hexahedron are jointed together, an octahedron is generated.
- On the contrary, if the mid-points of adjacent faces of an octahedron are jointed together, a hexahedron is generated.

As shown in Fig. 4, the regular hexahedron and octahedron have the same symmetry operations. By application of any of the symmetry operations, the structure remains the same physical appearance. For a regular hexahedron or octahedron, there exist 6 two-fold C_2' rotation axes, 4 three-fold C_3 rotation axes, and 3 four-fold C_4 rotation axes including 3 coincident two-fold C_2 rotation axes:

- Two-fold rotation axes C_2': The C_2' axes pass through the mid-points of pairs of opposite edges of the hexahedron or octahedron as well.
- Three-fold rotation axes C_3: Each C_3 axis passes through opposite pairs of vertices of the hexahedron, or mid-points of a pair of equilateral triangular faces on opposite sides of the octahedron.

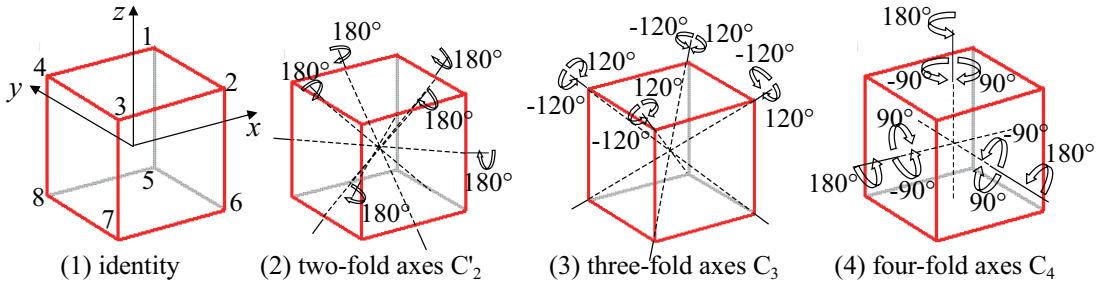

(a) symmetry operations of a regular hexahedron

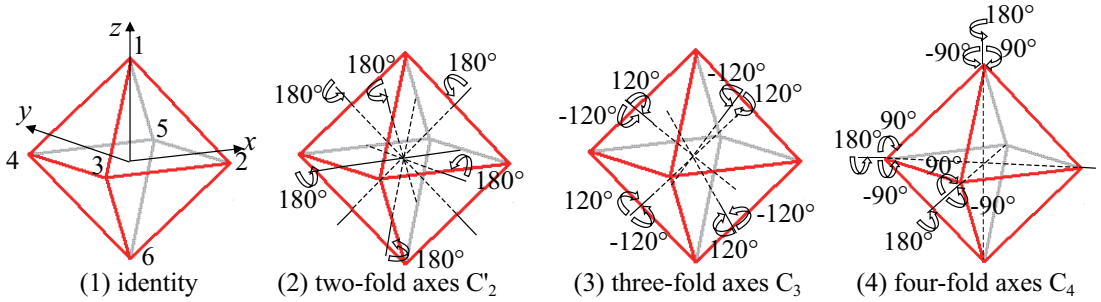

(b) symmetry operations of a regular octahedron

Fig. 4. Symmetry operations of the regular hexahedron and octahedron.

- Four-fold rotation axes C_4: The C_4 and the coincident C_2 axes pass through mid-points of a pair of square faces on opposite sides of the hexahedron, or opposite pairs of vertices of the octahedron.

Hence, there are in total 24 symmetry operations (rotations about the above-mentioned axes), including the identity operation doing nothing. These symmetry operations form the octahedral group, denoted by O. The octahedral group is a point group that has the order of 24. It is also the symmetry group of the hexahedron (cube), cuboctahedron, and truncated octahedron.

According to the coordinate system with the origin at the center as indicated in Fig. 4, coordinates of the vertices of the regular hexahedron are given as follows:

$$
\begin{aligned}
P_1 &= \begin{pmatrix} 1 \\ 1 \\ 1 \end{pmatrix}, \quad P_2 = \begin{pmatrix} 1 \\ -1 \\ 1 \end{pmatrix}, \quad P_3 = \begin{pmatrix} -1 \\ -1 \\ 1 \end{pmatrix}, \quad P_4 = \begin{pmatrix} -1 \\ 1 \\ 1 \end{pmatrix}, \\
P_5 &= \begin{pmatrix} 1 \\ 1 \\ -1 \end{pmatrix}, \quad P_6 = \begin{pmatrix} 1 \\ -1 \\ -1 \end{pmatrix}, \quad P_7 = \begin{pmatrix} -1 \\ -1 \\ -1 \end{pmatrix}, \quad P_8 = \begin{pmatrix} -1 \\ 1 \\ -1 \end{pmatrix}.
\end{aligned} \tag{2}
$$

Morever, coordinates of the vertices of the regular octahedron are given as

Table 1
Character table for the octahedral group O.

O	E	$8C_3(\tau)$	$6C_4(\phi)$	$3C_2(\phi)$	$6C_2'(\sigma)$	
A_1	1	1	1	1	1	$(x^2+y^2+z^2)$
A_2	1	1	-1	1	-1	$\mathrm{sgn}(\nu)$
E	2	-1	0	2	0	$[1/\sqrt{3}(2z^2-x^2-y^2),(x^2-y^2)]$
T_1	3	0	1	-1	-1	(x,y,z)
T_2	3	0	-1	-1	1	(xy,yz,zx)

$$P_1=\begin{pmatrix}0\\0\\1\end{pmatrix},\quad P_2=\begin{pmatrix}0\\-1\\0\end{pmatrix},\quad P_3=\begin{pmatrix}1\\0\\0\end{pmatrix},$$
$$P_4=\begin{pmatrix}0\\1\\0\end{pmatrix},\quad P_5=\begin{pmatrix}-1\\0\\0\end{pmatrix},\quad P_6=\begin{pmatrix}0\\0\\-1\end{pmatrix}. \tag{3}$$

2.2 Octahedral group and its representation matrices

In the octahedral group O, there are 2 one-dimensional irreducible representations A_1 and A_2, 1 two-dimensional irreducible representation E, and 2 three-dimensional irreducible representation T_1, and T_2. The character table for the group O is given in Table 1.

Combination of any two operations of a group must coincide with an operation of that group. The *group multiplication table* describes such combinations of any two operations in a group. If a set of matrices obeys the group multiplication table of a group, these matrices are said to form a matrix representation of that group. These matrices are called the *representation matrices*. A matrix representation that can be reduced to a linear combination (direct sum) of several matrix representations is called a reducible matrix representation, otherwise, they form an *irreducible matrix representation*. Moreover, *characters* are defined as traces of the irreducible representation matrices.

The (irreducible) representation matrices in the octahedral group can be generated by the generators A and B:

$$< A, B | A^2 = 1, B^3 = 1, (AB)^4 = 1 >, \tag{4}$$

where A refers to the two-fold rotation σ, B refers to the three-fould rotation τ, and the four-fold rotation ϕ can be generated by the multiplication of A and B.

As will be presented in the next section for derivation of the symmetry-adapted force density matrix, we need only the irrducible representation matrices for the members connected to the reference node. Hence, in the following, we present only the necessary irreducible representation matrices: $\rho^\mu(\mathrm{E})$ for the identity operation, $\rho^\mu(\sigma_{1,2})$ for the two-fold rotations σ_i $(i=1,2)$ about two C_2' axes, $\rho^\mu(\tau_{1,2})$ for the three-fold rotations τ_i $(i=1,2)$ about a C_3 axis, and $\rho^\mu(\phi_{1,2,3})$ for the four-fold rotations ϕ_i $(i=1,2,3)$ about a C_4 axis. Here, $\rho^\mu(\nu)$ denotes the matrix representation of symmetry operation ν correspondig to the representation μ.

Note that $\rho^\mu(\sigma_1)$ is used to describe the two-fold symmetry of edge cables, and $\rho^\mu(\sigma_2)$ is for the two-fold symmetry of struts. Furthermore, $\rho^E(\sigma_1)$ is adopted as the generator A

in Eq. (4) for the two-fold rotation, and $\rho^E(\tau_1)$ is used as the generator B in Eq. (4) for the three-fold rotation.

2.2.1 Irreducible representation matrices for A_1 and A_2

For the one-dimensional repsentations, there are unique choices since they are 1-by-1 matrices. From Table 1, we have the representation (one-by-one) matrices corresponding to the one-dimensional representation $(\mu =)A_1$ are all equal to one; i.e.,

$$\rho^{A_1}(\mathrm{E}) = \rho^{A_1}(\tau_{1,2}) = \rho^{A_1}(\phi_{1,2,3}) = \rho^{A_1}(\sigma_{1,2}) = 1. \tag{5}$$

Similarly, for the other one-dimensional representations A_2, their (one-by-one) representation matrices corresponding to each symmetry operation can be directly read off from Table 1:

$$\begin{aligned} \rho^{A_2}(\mathrm{E}) = \rho^{A_2}(\tau_{1,2}) = \rho^{A_2}(\phi_2) = 1, \\ \rho^{A_2}(\phi_{1,3}) = \rho^{A_2}(\sigma_{1,2}) = -1. \end{aligned} \tag{6}$$

2.2.2 Irreducible representation matrices for E

For the two-dimensional and three-dimensional repsentation matrices, they are not unique since they are dependent upon the coordinate system. The representation matrices presented in the following correspond to the selected coordinate system as indicated in Fig. 3, and the coordinates of the vertices of the hexhedron and octahedron were respectively given in Eqs. (2) and (3).

The representation matrix $\rho^E(\mathrm{E})$ corresponding to the two-dimensional representation E for the identity operation is an identity matrix:

$$\rho^E(\mathrm{E}) = \begin{pmatrix} 1 & 0 \\ 0 & 1 \end{pmatrix}, \tag{7}$$

the trace of which is

$$\mathrm{tr}(\rho^E(\mathrm{E})) = 2. \tag{8}$$

The representation matrix $\rho^E(\sigma_1)$ and $\rho^E(\sigma_2)$ for the two-fold rotations C_2' are given as

$$\begin{aligned} \rho^E(\sigma_1) &= \begin{pmatrix} 1 & 0 \\ 0 & -1 \end{pmatrix}, \\ \rho^E(\sigma_2) &= \frac{1}{2}\begin{pmatrix} -1 & -1 \\ -3 & 1 \end{pmatrix}. \end{aligned} \tag{9}$$

Traces of both of the matrices $\rho^E(\sigma_1)$ and $\rho^E(\sigma_2)$ are 0:

$$\mathrm{tr}(\rho^E(\sigma_{1,2})) = 0, \tag{10}$$

satisfying the character table in Table 1.

The generator $\rho^E(\tau_1)$ for the three-fold rotation C_3 is

$$\rho^E(\tau_1) = \frac{1}{2}\begin{pmatrix} -1 & 1 \\ -3 & -1 \end{pmatrix}, \tag{11}$$

from which we have the other three-fold rotation sharing the same rotation axis as

$$\rho^E(\tau_2) = \rho^E(\tau_1) \cdot \rho^E(\tau_1) = \frac{1}{2}\begin{pmatrix} -1 & -1 \\ 3 & -1 \end{pmatrix}. \tag{12}$$

The traces of $\rho^E(\tau_1)$ and $\rho^E(\tau_2)$ are

$$\mathrm{tr}(\rho^E(\tau_{1,2})) = -1. \tag{13}$$

From Eq. (4), the representation matrix $\rho^E(\phi_1)$ for the four-fold rotation C_4 is generated as

$$\rho^E(\phi_1) = \rho^E(\sigma_1) \cdot \rho^E(\tau_1) = \frac{1}{2}\begin{pmatrix} -1 & 1 \\ 3 & 1 \end{pmatrix}, \tag{14}$$

and the other two representation matrices of the four-fold rotation sharing the same axis are given as

$$\begin{aligned} \rho^E(\phi_2) &= \rho^E(\phi_1) \cdot \rho^E(\phi_1) = \begin{pmatrix} 1 & 0 \\ 0 & 1 \end{pmatrix}, \\ \rho^E(\phi_3) &= \rho^E(\phi_1) \cdot \rho^E(\phi_1) \cdot \rho^E(\phi_1) = \frac{1}{2}\begin{pmatrix} -1 & 1 \\ 3 & 1 \end{pmatrix}. \end{aligned} \tag{15}$$

The traces of these representation matrices for three-fold rotations are

$$\mathrm{tr}(\rho^E(\phi_{1,3})) = 0, \quad \mathrm{tr}(\rho^E(\phi_2)) = 2. \tag{16}$$

2.2.3 Irreducible representation matrices for T_1

The representation matrix $\rho^{T_1}(\mathrm{E})$ corresponding to the three-dimensional representation T_1 for the identity operation is

$$\rho^{T_1}(\mathrm{E}) = \begin{pmatrix} 1 & 0 & 0 \\ 0 & 1 & 0 \\ 0 & 0 & 1 \end{pmatrix}, \tag{17}$$

the trace of which is

$$\mathrm{tr}(\rho^{T_1}(\mathrm{E})) = 3. \tag{18}$$

The following representation matrix $\rho^{T_1}(\sigma_1)$ for the two-fold rotations C_2' is the generator A in Eq. (4):

$$\rho^{T_1}(\sigma_1) = \begin{pmatrix} 0 & 0 & 1 \\ 0 & -1 & 0 \\ 1 & 0 & 0 \end{pmatrix}, \tag{19}$$

which is also used to describe the two-fold symmetry of edge cables; moreover, the following representation matrix $\rho^{T_1}(\sigma_1)$ for the two-fold rotations C_2' is used to describe the two-fold symmetry of struts:

$$\rho^{T_1}(\sigma_2) = \begin{pmatrix} -1 & 0 & 0 \\ 0 & 0 & 1 \\ 0 & 1 & 0 \end{pmatrix}. \tag{20}$$

Both of the matrices $\rho^{T_1}(\sigma_1)$ and $\rho^{T_1}(\sigma_2)$ have the trace -1; i.e.,

$$\mathrm{tr}(\rho^{T_1}(\sigma_{1,2})) = -1, \tag{21}$$

satisfying the character table in Table 1.

The following representation matrices $\rho^{T_1}(\tau_1)$ for the three-fold rotation C_3 is used as the generator B in Eq. (4):

$$\rho^{T_1}(\tau_1) = \begin{pmatrix} 0 & 0 & 1 \\ 1 & 0 & 0 \\ 0 & 1 & 0 \end{pmatrix}, \tag{22}$$

from which we have the other three-fold rotation sharing the same rotation axis

$$\rho^{T_1}(\tau_2) = \rho^{T_1}(\tau_1) \cdot \rho^{T_1}(\tau_1) = \begin{pmatrix} 0 & 1 & 0 \\ 0 & 0 & 1 \\ 1 & 0 & 0 \end{pmatrix}. \tag{23}$$

The traces of $\rho^{T_1}(\tau_1)$ and $\rho^{T_1}(\tau_2)$ are

$$\mathrm{tr}(\rho^{T_1}(\tau_{1,2})) = 0. \tag{24}$$

From Eq. (4), the representation matrix $\rho^{T_1}(\phi_1)$ for the four-fold rotation C_4 is generated as

$$\rho^{T_1}(\phi_1) = \rho^{T_1}(\sigma_1) \cdot \rho^{T_1}(\tau_1) = \begin{pmatrix} 0 & -1 & 0 \\ 1 & 0 & 0 \\ 0 & 0 & 1 \end{pmatrix}, \tag{25}$$

and the other two representation matrices of the four-fold rotation sharing the same axis are given as

$$\begin{aligned} \rho^{T_1}(\phi_2) &= \rho^{T_1}(\phi_1) \cdot \rho^{T_1}(\phi_1) = \begin{pmatrix} -1 & 0 & 0 \\ 0 & -1 & 0 \\ 0 & 0 & 1 \end{pmatrix}, \\ \rho^{T_1}(\phi_3) &= \rho^{T_1}(\phi_1) \cdot \rho^{T_1}(\phi_1) \cdot \rho^{T_1}(\phi_1) = \begin{pmatrix} 0 & 1 & 0 \\ -1 & 0 & 0 \\ 0 & 0 & 1 \end{pmatrix}. \end{aligned} \tag{26}$$

The traces of these matrices are

$$\mathrm{tr}(\rho^{T_1}(\phi_{1,3})) = 1, \quad \mathrm{tr}(\rho^{T_1}(\phi_2)) = -1. \tag{27}$$

2.2.4 Irreducible representation matrices for T_2

Since the representations $\rho^{T_1}(\nu)$ of T_1 and $\rho^{T_2}(\nu)$ of T_2 satisfy

$$\rho^{T_2}(\nu) = \mathrm{sgn}(\nu)\rho^{T_1}(\nu) = \rho^{A_2}(\nu)\rho^{T_1}(\nu), \tag{28}$$

where $\mathrm{sgn}(\nu)$ for each representation can be found in the character table in Table 1 for the A_2 representation.

The representation matrix $\rho^{T_2}(\mathrm{E})$ corresponding to the identity operation E for the three-dimensional representation T_2 is

$$\rho^{T_2}(\mathrm{E}) = \rho^{A_2}(\mathrm{E})\rho^{T_1}(\mathrm{E}) = \rho^{T_1}(\mathrm{E}) = \begin{pmatrix} 1 & 0 & 0 \\ 0 & 1 & 0 \\ 0 & 0 & 1 \end{pmatrix}. \tag{29}$$

Similarly, for the three-fold rotations C_3, we have their representation matrices $\rho^{T_2}(\tau_i)$ as

$$\rho^{T_2}(\tau_i) = \rho^{T_1}(\tau_i), \quad i = 1, 2; \tag{30}$$

because from the characters corresponding to the three-fold rotations C_3 of A_2 representation in Table 1 we know that

$$\mathrm{sgn}(\tau_i) = \rho^{A_2}(\tau_i) = 1. \tag{31}$$

Thus, we further have

$$\mathrm{tr}(\rho^{T_2}(\tau_1)) = \mathrm{tr}(\rho^{T_1}(\tau_2)) = 0. \tag{32}$$

For the four-fold rotations C_4, we have two cases: the pure four-fold rotations C_4 and the corresponding two-fold rotations C_2, where

$$\begin{aligned} &\mathrm{sgn}(\phi_i) = -1, \quad i = 1, 3; \\ &\mathrm{sgn}(\phi_2) = 1. \end{aligned} \tag{33}$$

Thus, their irreducible representation matrices for T_2 are given as

$$\begin{aligned} &\rho^{T_2}(\phi_i) = -\rho^{T_1}(\phi_i), \quad i = 1, 3; \\ &\rho^{T_2}(\phi_2) = \rho^{T_1}(\phi_2). \end{aligned} \tag{34}$$

and their traces are

$$\mathrm{tr}(\rho^{T_2}(\phi_i)) = -1, \quad i = 1, 2, 3. \tag{35}$$

Moreover, for the pure two-fold rotations C_2', the representation matrices $\rho^{T_2}(\sigma_i)$ of T_2 are

$$\rho^{T_2}(\sigma_i) = \mathrm{sgn}(\sigma_i)\rho^{T_1}(\sigma_i) = -\rho^{T_1}(\sigma_i), \quad i = 1, 2, \tag{36}$$

and therefore, their traces are

$$\mathrm{tr}(\rho^{T_2}(\sigma_i)) = -\mathrm{tr}(\rho^{T_1}(\sigma_i)) = 1, \quad i = 1, 2. \tag{37}$$

3. Symmetry-adapted Force Density Matrix

The conditions for self-equilibrium and super-stability of a tensegrity structure can be found by respectively investigating the nullities and positive-definiteness of its force density matrix. For such purpose, we present the analytical symmetry-adapted (block-diagonalized) force density matrix in this section.

3.1 Force density matrix

The force density matrix of a structure is determined only by connectivity pattern as well as force densities of the members. The term *force density* is defined as the ratio of prestress to member length. It was initially introduced by Schek (1974) to transform the originally nonlinear equilibrium equations into linear equations with respect to nodal coordinates for self-equilibrium analysis of cable nets.

Denoting by $\mathcal{I}$ the set of members connected to node i, the (i,j)-component $E_{(i,j)}$ of the force density matrix $\mathbf{E}$ is given as

$$E_{(i,j)} = \begin{cases} \sum\limits_{k\in\mathcal{I}} q_k & \text{for } i = j, \\ -q_k & \text{if nodes } i \text{ and } j \text{ are connected by member } k, \\ 0 & \text{for other cases,} \end{cases} \tag{38}$$

where q_k is the force density of member k connecting nodes i and j. Obviously, the force density matrix is symmetric, and thus, has real eigenvalues.

The self-equilibrium equations of a tensegrity structure can be written as follows with respect to the nodal coordinates $\mathbf{x}$, $\mathbf{y}$, $\mathbf{z}$:

$$\mathbf{Ex} = \mathbf{Ey} = \mathbf{Ez} = \mathbf{0}, \tag{39}$$

where $\mathbf{0}$ indicates that there is no external loads applied at the structure.

Tensegrity structures are generally *free-standing*; i.e., any boundary conditions are not imposed to constrain the rigid-body motions. Hence, there exists no fixed node in a tensegrity structure, and sum of the entries in each row or each column of the force density matrix is zero. Thus, the force density matrix has nullity of at lease one, or equivalently, the matrix has at least one zero eigenvalue. In fact, it has more nullities: Zhang and Ohsaki (2015) discussed that the force density matrix should have nullities of at least four for a non-degenerate tensegrity structure in three-dimensional space. This is to ensure that the geometry realization of a tensegrity structure, in terms of nodal coordinates $\mathbf{x}$, $\mathbf{y}$, and $\mathbf{z}$, has non-trivial solutions for the self-equilibrium equations in Eq. (39) (Zhang and Ohsaki, 2006).

3.2 Stability and super-stability

In the traditional stability theory in engineering, a structure is stable if its (tangent) stiffness matrix is positive definite, while the rigid-body motions have been properly constrained; i.e., the quadratic form of the tangent stiffness matrix with respect to any non-trivial motion, excluding the rigid-body motions, is positive (Thompson and Hunt, 1984). The tangent stiffness matrix $\mathbf{K}$ is the sum of the linear stiffness matrix $\mathbf{K}_{\mathrm{E}}$ and the geometrical stiffness matrix $\mathbf{K}_{\mathrm{G}}$:

$$\mathbf{K} = \mathbf{K}_{\mathrm{E}} + \mathbf{K}_{\mathrm{G}}. \tag{40}$$

Moreover, $\mathbf{K}_{\mathrm{G}}$ is composed of the force density matrix (Guest, 2006; Zhang and Ohsaki, 2006):

$$\mathbf{K}_{\mathrm{G}} = \mathbf{E} \oplus \mathbf{E} \oplus \mathbf{E}, \tag{41}$$

where the notation $\oplus$ indicates that three copies of $\mathbf{E}$ are lying on the leading diagonal of $\mathbf{K}_{\mathrm{G}}$.

Since the force density matrix $\mathbf{E}$ has more than four zero eigenvalues, the geometrical stiffness matrix $\mathbf{K}_{\mathrm{G}}$ has more than 12 zero eigenvalues for a three-dimensional tensegrity. Among these, six of the zero eigenvalues in $\mathbf{K}_{\mathrm{G}}$ correspond to the rigid-body motions of the structures, and the other six correspond to the non-trivial affine motions (Zhang and Ohsaki, 2007).

It is notable that the geometrical stiffness matrix (or the force density matrix) is only relevant to (level and distribution of) prestress. Increasing the prestress level would increase or decrease the geometrical stiffness depending on property of $\mathbf{K}_{\mathrm{G}}$: If $\mathbf{K}_{\mathrm{G}}$ is positive semi-definite, then increasing prestress level will increase the (geometrical) stiffness of the structure; If there exists negative eigenvalues in $\mathbf{K}_{\mathrm{G}}$, high level of prestress could decrease the (geometrical) stiffness, and even results in an unstable structure. Hence, positive semi-definiteness of $\mathbf{K}_{\mathrm{G}}$ or $\mathbf{E}$ is the necessary condition for super-stability of tensegrity structures (Connelly and Back, 1998; Zhang and Ohsaki, 2007). A super-stable structure is always stable irrespective of material properties as well as the level of prestress.

Regarding the six non-trivial affine motions, they result in zero quadratic form of $\mathbf{K}_{\mathrm{G}}$ because the affine motions lie in the null space of $\mathbf{K}_{\mathrm{G}}$. Hence, the quadratic form of $\mathbf{K}_{\mathrm{E}}$ with respect to the affine motions should not be zero to ensure a stable structure. This is guaranteed by full rank of the geometry matrix as discussed by Zhang and Ohsaki (2007).

To guarantee a super-stable tensegrity structure, Zhang and Ohsaki (2007) presented the following three sufficient conditions:

(1) The geometry matrix of the structure has rank of six for a three-dimensional structure, or equivalently, the member directions do not lie on the same conic at infinity (Connelly, 1999);
(2) The force density matrix is positive semi-definite;
(3) The force density matrix has minimum number of nullities, which is four for a three-dimensional tensegrity structure.

In the following, we will concentrate only on the last two conditions in the super-stability investigation, since the first condition is usually satisfied (Zhang and Ohsaki, 2007). Furthermore, both of the number of nullities and positive (semi-)definiteness of a matrix are directly related to its eigenvalues. Hence, self-equilibrium analysis as well as stability investigation of a tensegrity structure can be conducted by studying the eigenvalues of the force density matrix.

3.3 Symmetry-adapted structure

By making use of symmetry properties of the structure, self-equilibrium analysis and stability investigation become much easier since the force density matrix is rearranged in a symmetry-adapted form, with the independent sub-matrices lying on the leading diagonal. Eigenvalues of the force density matrix can then be calculated by using these sub-matrices with much smaller size than the original matrix.

The block (sub-matrix) $\tilde{\mathbf{E}}^{\mu}$ of the symmetry-adapted force density matrix $\tilde{\mathbf{E}}$ corresponding to the representation μ can be obtained by applying (coordinate) transformation matrices on both sides of the original force density matrix. A (stiffness) matrix can be block-diagonalized by using numerical methods (Ikeda and Murota, 1991; Kangwai *et al.*,

1999).

To present the analytical conditions for self-equilibrium as well as super-stability of the hexahedral and octahedral structures, we follow the analytical procedure proposed by Zhang *et al.* (2009b) for block-diagonalization of the force density matrix, directly using the irreducible representation matrices. This analytical method based on group representation theory can be directly applied to any symmetric structures, as long as the nodes belong to a single regular orbit; i.e., positions of the nodes can be exchanged by another node by application of one proper symmetry operation of the group. For the structures with multiple orbits or non-regular orbit of nodes, e.g., the star-shaped structures (Zhang *et al.*, 2010) with two orbits of nodes, special techniques are necessary to block-diagonalize the force density matrix.

Since any symmetry operation of a regular hexahedron or octahedron, except the identity operation E, will exchange positions of the nodes, we have the numbers of nodes that will not change their positions by the corresponding symmetry operations as

Symmetry operation:	E	$8\mathrm{C}_3(\tau)$	$6\mathrm{C}_4(\phi)$	$3\mathrm{C}_2(\phi)$	$6\mathrm{C}_2'(\sigma)$
Number of unchanged nodes:	24	0	0	0	0

(42)

From characters of the irreducible representations of octahedral group as listed in Table 1, the reducible representation $\Gamma(N)$ of the nodes can be written as a linear combination of the irreducible representations in a general form as

$$\Gamma(N) = A_1 + A_2 + 2E + 3T_1 + 3T_2. \tag{43}$$

Eq. (43) comes from the fact that sum of the characters of the representations corresponding to each symmetry operation is equal to the number of unchanged nodes:

	E	$8\mathrm{C}_3(\tau)$	$6\mathrm{C}_4(\phi)$	$3\mathrm{C}_2(\phi)$	$6\mathrm{C}_2'(\sigma)$
A_1	1	1	1	1	1
A_2	1	1	-1	1	-1
$2E$	4	-2	0	4	0
$3T_1$	9	0	3	-3	-3
$3T_2$	9	0	-3	-3	3
$=$	24	0	0	0	0

(44)

The linear combination of representations for nodes characterizes the structure of the symmetry-adapted force density matrix $\tilde{\mathbf{E}}$, where $\tilde{(\cdot)}$ is used to denote the symmetry-adapted form of a matrix: there are

- 1 one-dimensional block $\tilde{\mathbf{E}}^{A_1}$ corresponding to representation A_1,
- 1 one-dimensional block $\tilde{\mathbf{E}}^{A_2}$ corresponding to representation A_2,
- 2 copies of the two-dimensional block $\tilde{\mathbf{E}}^{E}$ corresponding to representation E,
- 3 copies of the three-dimensional block $\tilde{\mathbf{E}}^{T_1}$ corresponding to representation T_1, and
- 3 copies of the three-dimensional block $\tilde{\mathbf{E}}^{T_2}$ corresponding to representation T_2.

Hence, the structure of $\tilde{\mathbf{E}}$ can be summarized as follows, with the independent sub-

matrices $\tilde{\mathbf{E}}^{\mu}$ lying on the leading diagonal

$$\underset{24\times24}{\tilde{\mathbf{E}}} = \underset{1\times1}{\tilde{\mathbf{E}}^{A_1}} \oplus \underset{1\times1}{\tilde{\mathbf{E}}^{A_2}} \oplus 2\underset{2\times2}{\tilde{\mathbf{E}}^{E}} \oplus 3\underset{3\times3}{\tilde{\mathbf{E}}^{T_1}} \oplus 3\underset{3\times3}{\tilde{\mathbf{E}}^{T_2}}. \tag{45}$$

3.4 Symmetry-adapted blocks

The members of a hexahedral or octahedral structure are classified into three types: edge cables, cutting cables, and struts. Each type of members has the same force density according to symmetry, which are denoted by q_{e}, q_{c}, and q_{s}, respectively.

Because each (reference) node of the structure is connected by only one edge cable, the reference node moves to the same position of the other end of the edge cable, no matter it is rotated by the angles θ or $-\theta$ about a specified rotation axis. Thus, the rotation angle θ can only be π, or $-\pi$. This is indeed the two-fold rotation C_2' denoted by σ_1. Similarly, the two nodes connecting to a strut can exchange their positions by another two-fold rotation σ_2.

On the other hand, each node of the structure is connected by two cutting cables, and the rotation angle θ is less than π. Hence, the reference node is connected to the nodes according to the three-fold rotations τ_1 and τ_2 in the case of hexahedral symmetry; and it is connected to the nodes according to two of the four-fold rotations ϕ_1 and ϕ_3 in the case of octahedral symmetry.

Because the nodes of a hexahedral or octahedral structure belong to a regular orbit, the sub-matrices corresponding to each distinct representation are formulated as sum of the multiplication of irreducible representation matrices and force densities connected to the reference node (Zhang *et al.*, 2009b). Accordingly, the sub-matrix $\tilde{\mathbf{E}}^{\mu}$ corresponding to representation μ can be written in a general form as follows:

- For the hexahedral structure, $\tilde{\mathbf{E}}_{\mathrm{H}}^{\mu}$ is given as

$$\tilde{\mathbf{E}}_{\mathrm{H}}^{\mu} = (2q_{\mathrm{c}} + q_{\mathrm{e}} + q_{\mathrm{s}})\rho^{\mu}(\mathrm{E}) - q_{\mathrm{c}}\rho^{\mu}(\tau_1) - q_{\mathrm{c}}\rho^{\mu}(\tau_2) - q_{\mathrm{e}}\rho^{\mu}(\sigma_1) - q_{\mathrm{s}}\rho^{\mu}(\sigma_2). \tag{46}$$

- For the octahedral structure, $\tilde{\mathbf{E}}_{\mathrm{O}}^{\mu}$ is given as

$$\tilde{\mathbf{E}}_{\mathrm{O}}^{\mu} = (2q_{\mathrm{c}} + q_{\mathrm{e}} + q_{\mathrm{s}})\rho^{\mu}(\mathrm{E}) - q_{\mathrm{c}}\rho^{\mu}(\phi_1) - q_{\mathrm{c}}\rho^{\mu}(\phi_3) - q_{\mathrm{e}}\rho^{\mu}(\sigma_1) - q_{\mathrm{s}}\rho^{\mu}(\sigma_2). \tag{47}$$

3.4.5 One-dimensional blocks $\tilde{\mathbf{E}}^{A_1}$ and $\tilde{\mathbf{E}}^{A_2}$

According to Eq. (46), Eq. (47), and Table 1, we have the one-dimensional blocks $\tilde{\mathbf{E}}_{\mathrm{H}}^{A_1}$ and $\tilde{\mathbf{E}}_{\mathrm{O}}^{A_1}$ for the one-dimensional representation A_1 as

$$\tilde{\mathbf{E}}_{\mathrm{H}}^{A_1} = \tilde{\mathbf{E}}_{\mathrm{O}}^{A_1} = (2q_{\mathrm{c}} + q_{\mathrm{e}} + q_{\mathrm{s}}) - q_{\mathrm{c}} - q_{\mathrm{c}} - q_{\mathrm{e}} - q_{\mathrm{s}} = 0, \tag{48}$$

which indicates that $\tilde{\mathbf{E}}_{\mathrm{H}}^{A_1}$ and $\tilde{\mathbf{E}}_{\mathrm{O}}^{A_1}$ are always zero.

For the other one-dimensional representations A_2, the one-dimensional block $\tilde{\mathbf{E}}_{\mathrm{H}}^{A_2}$ for the hexahedral structure is

$$\tilde{\mathbf{E}}_{\mathrm{H}}^{A_2} = (2q_{\mathrm{c}} + q_{\mathrm{e}} + q_{\mathrm{s}}) - q_{\mathrm{c}} - q_{\mathrm{c}} - (-1)q_{\mathrm{e}} - (-1)q_{\mathrm{s}} = 2(q_{\mathrm{e}} + q_{\mathrm{s}}), \tag{49}$$

and the one-dimensional block $\tilde{\mathbf{E}}_{\mathrm{H}}^{A_2}$ for the octahedral structure is

$$\tilde{\mathbf{E}}_{\mathrm{O}}^{A_2} = (2q_{\mathrm{c}} + q_{\mathrm{e}} + q_{\mathrm{s}}) - (-1)q_{\mathrm{c}} - (-1)q_{\mathrm{c}} - (-1)q_{\mathrm{e}} - (-1)q_{\mathrm{s}} = 4q_{\mathrm{c}} + 2q_{\mathrm{e}} + 2q_{\mathrm{s}}. \tag{50}$$

3.4.6 Two-dimensional block $\tilde{\mathbf{E}}^{E}$

The two-dimensional block $\tilde{\mathbf{E}}_{\mathrm{H}}^{E}$ of the hexahedral structure corresponding to E representation is

$$\begin{aligned}\tilde{\mathbf{E}}_{\mathrm{H}}^{E} &= (2q_{\mathrm{c}} + q_{\mathrm{e}} + q_{\mathrm{s}})\rho^{E}(\mathrm{E}) - q_{\mathrm{c}}\rho^{E}(\tau_1) - q_{\mathrm{c}}\rho^{E}(\tau_2) - q_{\mathrm{e}}\rho^{E}(\sigma_1) - q_{\mathrm{s}}\rho^{E}(\sigma_2) \\ &= \begin{pmatrix} 3q_{\mathrm{c}} + 3q_{\mathrm{s}}/2 & q_2/2 \\ 3q_{\mathrm{s}}/2 & 3q_{\mathrm{c}} + 2q_{\mathrm{e}} + q_{\mathrm{s}}/2 \end{pmatrix}.\end{aligned} \tag{51}$$

The two-dimensional block $\tilde{\mathbf{E}}_{\mathrm{O}}^{E}$ of the octahedral structure corresponding to E representation is

$$\begin{aligned}\tilde{\mathbf{E}}_{\mathrm{O}}^{E} &= (2q_{\mathrm{c}} + q_{\mathrm{e}} + q_{\mathrm{s}})\rho^{E}(\mathrm{E}) - q_{\mathrm{c}}\rho^{E}(\phi_1) - q_{\mathrm{c}}\rho^{E}(\phi_3) - q_{\mathrm{e}}\rho^{E}(\sigma_1) - q_{\mathrm{s}}\rho^{E}(\sigma_2) \\ &= \begin{pmatrix} 3q_{\mathrm{c}} + 3q_{\mathrm{s}}/2 & -q_{\mathrm{c}} + q_2/2 \\ -3q_{\mathrm{c}} + 3q_{\mathrm{s}}/2 & q_{\mathrm{c}} + 2q_{\mathrm{e}} + q_{\mathrm{s}}/2 \end{pmatrix}.\end{aligned} \tag{52}$$

3.4.7 Three-dimensional block $\tilde{\mathbf{E}}^{T_1}$

The three-dimensional block $\tilde{\mathbf{E}}_{\mathrm{H}}^{T_1}$ of the hexahedral structure corresponding to T_1 representation is

$$\begin{aligned}\tilde{\mathbf{E}}_{\mathrm{H}}^{T_1} &= (2q_{\mathrm{c}} + q_{\mathrm{e}} + q_{\mathrm{s}})\rho^{T_1}(\mathrm{E}) - q_{\mathrm{c}}\rho^{T_1}(\tau_1) - q_{\mathrm{c}}\rho^{T_1}(\tau_2) - q_{\mathrm{e}}\rho^{T_1}(\sigma_1) - q_{\mathrm{s}}\rho^{T_1}(\sigma_2) \\ &= \begin{pmatrix} 2q_{\mathrm{c}} + q_{\mathrm{e}} + 2q_{\mathrm{s}} & -q_{\mathrm{c}} & -q_{\mathrm{c}} - q_{\mathrm{e}} \\ -q_{\mathrm{c}} & 2q_{\mathrm{c}} + 2q_{\mathrm{e}} + q_{\mathrm{s}} & -q_{\mathrm{c}} - q_{\mathrm{s}} \\ -q_{\mathrm{c}} - q_{\mathrm{e}} & -q_{\mathrm{c}} - q_{\mathrm{s}} & 2q_{\mathrm{c}} + q_{\mathrm{e}} + q_{\mathrm{s}} \end{pmatrix}.\end{aligned} \tag{53}$$

The three-dimensional block $\tilde{\mathbf{E}}_{\mathrm{O}}^{T_1}$ of the octahedral structure corresponding to T_1 representation is

$$\begin{aligned}\tilde{\mathbf{E}}_{\mathrm{O}}^{T_1} &= (2q_{\mathrm{c}} + q_{\mathrm{e}} + q_{\mathrm{s}})\rho^{T_1}(\mathrm{E}) - q_{\mathrm{c}}\rho^{T_1}(\phi_1) - q_{\mathrm{c}}\rho^{T_1}(\phi_3) - q_{\mathrm{e}}\rho^{T_1}(\sigma_1) - q_{\mathrm{s}}\rho^{T_1}(\sigma_2) \\ &= \begin{pmatrix} 2q_{\mathrm{c}} + q_{\mathrm{e}} + 2q_{\mathrm{s}} & 0 & -q_{\mathrm{e}} \\ 0 & 2q_{\mathrm{c}} + 2q_{\mathrm{e}} + q_{\mathrm{s}} & -q_{\mathrm{s}} \\ -q_{\mathrm{e}} & -q_{\mathrm{s}} & q_{\mathrm{e}} + q_{\mathrm{s}} \end{pmatrix}.\end{aligned} \tag{54}$$

3.4.8 Three-dimensional block $\tilde{\mathbf{E}}^{T_2}$

The three-dimensional block $\tilde{\mathbf{E}}_{\mathrm{H}}^{T_2}$ of the hexahedral structure corresponding to T_2 representation is

$$\begin{aligned}\tilde{\mathbf{E}}_{\mathrm{H}}^{T_2} &= (2q_{\mathrm{c}} + q_{\mathrm{e}} + q_{\mathrm{s}})\rho^{T_2}(\mathrm{E}) - q_{\mathrm{c}}\rho^{T_2}(\tau_1) - q_{\mathrm{c}}\rho^{T_2}(\tau_2) - q_{\mathrm{e}}\rho^{T_2}(\sigma_1) - q_{\mathrm{s}}\rho^{T_2}(\sigma_2) \\ &= \begin{pmatrix} 2q_{\mathrm{c}} + q_{\mathrm{e}} & -q_{\mathrm{c}} & -q_{\mathrm{c}} + q_{\mathrm{e}} \\ -q_{\mathrm{c}} & 2q_{\mathrm{c}} + q_{\mathrm{s}} & -q_{\mathrm{c}} + q_{\mathrm{s}} \\ -q_{\mathrm{c}} + q_{\mathrm{e}} & -q_{\mathrm{c}} + q_{\mathrm{s}} & 2q_{\mathrm{c}} + q_{\mathrm{e}} + q_{\mathrm{s}} \end{pmatrix}.\end{aligned} \tag{55}$$

The three-dimensional block $\tilde{\mathbf{E}}_{\mathrm{O}}^{T_2}$ of the octahedral structure corresponding to T_2 representation is

$$\begin{aligned}\tilde{\mathbf{E}}_{\mathrm{O}}^{T_2} &= (2q_{\mathrm{c}}+q_{\mathrm{e}}+q_{\mathrm{s}})\rho^{T_2}(\mathrm{E}) - q_{\mathrm{c}}\rho^{T_2}(\phi_1) - q_{\mathrm{c}}\rho^{T_2}(\phi_3) - q_{\mathrm{e}}\rho^{T_2}(\sigma_1) - q_{\mathrm{s}}\rho^{T_2}(\sigma_2) \\ &= \begin{pmatrix} q_{\mathrm{e}}+q_{\mathrm{s}} & -q_{\mathrm{s}} & -q_{\mathrm{e}} \\ -q_{\mathrm{s}} & 2q_{\mathrm{c}}+q_{\mathrm{s}} & 0 \\ -q_{\mathrm{e}} & 0 & 2q_{\mathrm{c}}+q_{\mathrm{e}} \end{pmatrix}. \end{aligned} \tag{56}$$

4. Hexahedral Structures

This section presents the conditions for self-equilibrium as well as super-stability of the truncated regular hexahedral structure.

4.1 Self-equilibrium conditions

For the self-equilibrium of a tensegrity structure, its force density necessarily has four zero eigenvalues. In the symmetry-adapted form, there always exists one zero eigenvalue in $\tilde{\mathbf{E}}_{\mathrm{H}}^{A_1}$ as in Eq. (48). The other three zero eigenvalues come from the three copies of the three-dimensional block $\tilde{\mathbf{E}}_{\mathrm{H}}^{T_1}$, as also indicated in the character table.

Eigenvalues λ of $\tilde{\mathbf{E}}_{\mathrm{H}}^{T_1}$ are calculated by enforcing the following equation to zero

$$\begin{aligned}&\det(\tilde{\mathbf{E}}_{\mathrm{H}}^{T_1} - \lambda\mathbf{I}) \\ &= -\lambda[\lambda^2 - (6q_{\mathrm{c}}+4q_{\mathrm{e}}+4q_{\mathrm{s}})\lambda + 9q_{\mathrm{c}}^2 + 14(q_{\mathrm{e}}+q_{\mathrm{s}})q_{\mathrm{c}} + 4q_{\mathrm{e}}^2 + 4q_{\mathrm{s}}^2 + 11q_{\mathrm{e}}q_{\mathrm{s}}] \\ &\quad +2[3(q_{\mathrm{e}}+q_{\mathrm{s}})q_{\mathrm{c}}^2 + 2(q_{\mathrm{e}}^2+q_{\mathrm{s}}^2+4q_{\mathrm{e}}q_{\mathrm{s}})q_{\mathrm{c}} + 3q_{\mathrm{e}}q_{\mathrm{s}}(q_{\mathrm{e}}+q_{\mathrm{s}})] \\ &= 0. \end{aligned} \tag{57}$$

Having zero eigenvalue ($\lambda = 0$) means that

$$3(q_{\mathrm{e}}+q_{\mathrm{s}})q_{\mathrm{c}}^2 + 2(q_{\mathrm{e}}^2+q_{\mathrm{s}}^2+4q_{\mathrm{e}}q_{\mathrm{s}})q_{\mathrm{c}} + 3q_{\mathrm{e}}q_{\mathrm{s}}(q_{\mathrm{e}}+q_{\mathrm{s}}) = 0, \tag{58}$$

and the other (non-)zero eigenvalues are solved from the following equation

$$\lambda^2 - (6q_{\mathrm{c}}+4q_{\mathrm{e}}+4q_{\mathrm{s}})\lambda + 9q_{\mathrm{c}}^2 + 14(q_{\mathrm{e}}+q_{\mathrm{s}})q_{\mathrm{c}} + 4q_{\mathrm{e}}^2 + 4q_{\mathrm{s}}^2 + 11q_{\mathrm{e}}q_{\mathrm{s}} = 0. \tag{59}$$

Denoting

$$\begin{aligned} q_{\mathrm{e}} &= p + q \ (>0), \\ q_{\mathrm{s}} &= p - q \ (<0), \end{aligned} \tag{60}$$

we have

$$\begin{aligned} p &= \frac{q_{\mathrm{e}}+q_{\mathrm{s}}}{2}, \\ q &= \frac{q_{\mathrm{e}}-q_{\mathrm{s}}}{2} \ (>0). \end{aligned} \tag{61}$$

By using Eq. (61), Eq. (58) is rearranged as

$$6pq_{\mathrm{c}}^2 + (12p^2 - 4q^2)q_{\mathrm{c}} + 6p(p^2-q^2) = 0, \tag{62}$$

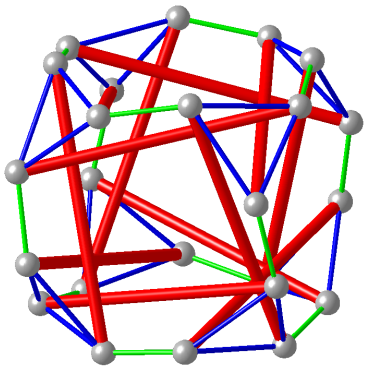

Fig. 5. Self-equilibrated configuration corresponding with $p = 1, q = 2$ or $q_e = 3, q_s = -1$.

which is solved as follows by considering the value of p:

- $p = 0$: The solution of Eq. (62) results in

$$q_c = 0, \tag{63}$$

  which is a trivial solution since the force (density q_c) of the cutting cables should be positive to carry tension. Thus, this case is ignored for further investigation.

- $p \neq 0$: The solution of Eq. (62) results in

$$\begin{aligned} q_{c1} &= \frac{(-3p^2 + q^2) + q\sqrt{3p^2 + q^2}}{3p}, \\ q_{c2} &= \frac{(-3p^2 + q^2) - q\sqrt{3p^2 + q^2}}{3p}. \end{aligned} \tag{64}$$

  From Eq. (60), we know that

$$q^2 - p^2 = -(p + q)(p - q) > 0, \tag{65}$$

  therefore, we have

$$(q\sqrt{3p^2 + q^2})^2 - (-3p^2 + q^2)^2 = 9p^2(q^2 - p^2) > 0. \tag{66}$$

  Hence, in order to ensure $q_c > 0$ for carrying tension in the cutting cables, we need to consider the following two cases

  · For $q_{c1} > 0$, we need

$$p > 0. \tag{67}$$

  · For $q_{c2} > 0$, we need

$$p < 0. \tag{68}$$

4.2 Super-stability condition

Except for the four zero eigenvalues in the (symmetr-adapted) force density matrix for self-equilibrium, all other eigenvalues have to be positive to guarantee super-stability.

According to Eq. (49), the one-dimensional block $\tilde{\mathbf{E}}_H^{A_2}$ becomes

$$\tilde{\mathbf{E}}_H^{A_2} = 2(q_e + q_s) = 2p. \tag{69}$$

To guarantee that the cutting cables carry tension and positive definiteness of $\tilde{\mathbf{E}}_{\mathrm{H}}^{A_2}$, $q_{\mathrm{c}1}$ in Eq. (67) with $p > 0$ is the only possible solution for cutting cables. Hereafter, we consider only this solution for the discussions on super-stability.

By solving Eq. (59), the two non-zero eigenvalues $\lambda_{2,3}^{T_1}$ of $\tilde{\mathbf{E}}_{\mathrm{H}}^{T_1}$ are calculated as

$$\lambda_{2,3}^{T_1} = (3q_{\mathrm{c}} + 2q_{\mathrm{e}} + 2q_{\mathrm{s}}) \pm \sqrt{-(2q_{\mathrm{c}}q_{\mathrm{e}} + 2q_{\mathrm{c}}q_{\mathrm{s}} + 3q_{\mathrm{e}}q_{\mathrm{s}})} = b \pm \sqrt{c}, \tag{70}$$

where

$$\begin{aligned} b &= 3q_{\mathrm{c}} + 2q_{\mathrm{e}} + 2q_{\mathrm{s}} = \frac{1}{p}(p^2 + q^2 + q\sqrt{3p^2 + q^2}), \\ c &= -(2q_{\mathrm{c}}q_{\mathrm{e}} + 2q_{\mathrm{c}}q_{\mathrm{s}} + 3q_{\mathrm{e}}q_{\mathrm{s}}) = \frac{1}{3}(3p^2 + 5q^2 - 4q\sqrt{3p^2 + q^2}). \end{aligned} \tag{71}$$

Since

$$(3p^2 + 5q^2)^2 - (4q\sqrt{3p^2 + q^2})^2 = 9(q^2 - p^2)^2, \tag{72}$$

and $q > p > 0$, we may conclude that $c > 0$. Moreover, the following inequality holds

$$\begin{aligned} b^2 - c &= \frac{1}{3p^2}(3q^4 + 3q^2\sqrt{3p^2 + q^2} + p^2q^2 + 10p^2q\sqrt{3p^2 + q^2} + 6q^3\sqrt{3p^2 + q^2}) \\ &> 0, \end{aligned} \tag{73}$$

because $q > p > 0$. Therefore, both of the eigenvalues $\lambda_{2,3}^{T_1}$ in Eq. (70) are positive.

Trace of $\tilde{\mathbf{E}}_{\mathrm{H}}^{E}$ given in Eq. (51) is equal to the sum of its eigenvalues

$$\begin{aligned} \mathrm{tr}(\tilde{\mathbf{E}}_{\mathrm{H}}^{E}) &= \lambda_1^E + \lambda_2^E \\ &= 6q_{\mathrm{c}} + 2q_{\mathrm{c}} + 2q_{\mathrm{s}} = 6q_{\mathrm{c}} + 4p \\ &> 0, \end{aligned} \tag{74}$$

since $p > 0$ for $q_{\mathrm{c}1}$. Moreover, determinant of $\tilde{\mathbf{E}}_{\mathrm{H}}^{E}$ is equal to multiplication of its eigenvalues

$$\begin{aligned} \det(\tilde{\mathbf{E}}_{\mathrm{H}}^{E}) &= \lambda_1^E\lambda_2^E \\ &= 9q_{\mathrm{e}}^2 + 6q_{\mathrm{e}}(q_{\mathrm{s}} + 6q_{\mathrm{e}}q_{\mathrm{c}}) + 3q_{\mathrm{s}}q_{\mathrm{c}} \\ &= 9q_{\mathrm{e}}^2 - 9p^2 + q^2 + 4q\sqrt{3p^2 + q^2} \\ &> 9q_{\mathrm{e}}^2 - 9p^2 + p^2 + 4q\sqrt{3p^2 + p^2} \\ &> 9q_{\mathrm{e}}^2 > 0, \end{aligned} \tag{75}$$

where $q^2 > p^2$ has been applied. Accordingly, the two-dimensional block $\tilde{\mathbf{E}}_{\mathrm{H}}^{E}$ must be positive definite.

Trace of $\tilde{\mathbf{E}}_{\mathrm{H}}^{T_2}$ given in Eq. (55) is equal to the sum of its eigenvalues

$$\begin{aligned} \mathrm{tr}(\tilde{\mathbf{E}}_{\mathrm{H}}^{T_2}) &= \lambda_1^{T_2} + \lambda_2^{T_2} + \lambda_3^{T_2} \\ &= 6q_{\mathrm{c}} + 2q_{\mathrm{c}} + 2q_{\mathrm{s}} = 6q_{\mathrm{c}} + 4p \\ &> 0. \end{aligned} \tag{76}$$

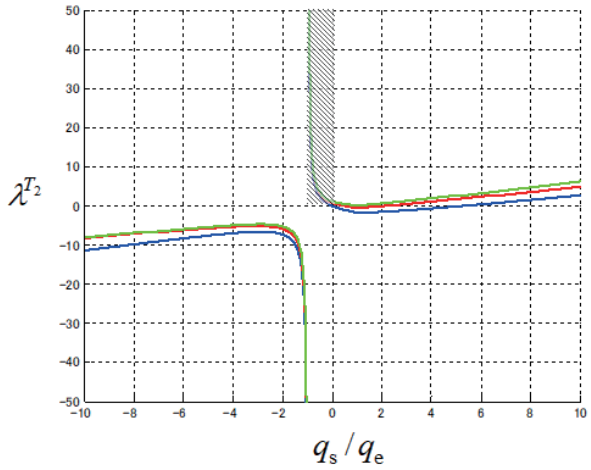

Fig. 6. Eigenvalues λ^{T_2} of $\tilde{\mathbf{E}}_{\mathrm{H}}^{T_2}$ with respect to $q_{\mathrm{s}}/q_{\mathrm{e}}$.

Moreover, determinant of $\tilde{\mathbf{E}}_{\mathrm{H}}^{T_2}$ is equal to multiplication of its eigenvalues

$$\begin{aligned}
\det(\tilde{\mathbf{E}}_{\mathrm{H}}^{T_2}) &= \lambda_1^{T_2}\lambda_2^{T_2}\lambda_3^{T_2} \\
&= 4q_{\mathrm{c}}(3q_{\mathrm{c}}q_{\mathrm{s}} + 3q_{\mathrm{c}}q_{\mathrm{e}} + 2q_{\mathrm{e}}q_{\mathrm{s}}) \\
&= 4q_{\mathrm{c}}(6q_{\mathrm{c}}p + 2p^2 - 2q^2) \\
&= 8q_{\mathrm{c}}(-2p^2 + q\sqrt{3p^2 + q^2}) \\
&> 8q_{\mathrm{c}}(-2p^2 + p\sqrt{3p^2 + p^2}) = 0,
\end{aligned} \tag{77}$$

where $q > p > 0$ has been applied. Accordingly, the three eigenvalues of $\tilde{\mathbf{E}}_{\mathrm{H}}^{T_2}$ are highly possible to be positive. Furthermore, its eigenvalues with respect to $q_{\mathrm{s}}/q_{\mathrm{e}}$ are plotted in Fig. 6. It can be observed that they are always positive in the shaded region where $-1 < q_{\mathrm{s}}/q_{\mathrm{e}} < 0$; or equivalently, $p = (q_{\mathrm{e}} - q_{\mathrm{s}})/2 > 0$.

5. Octahedral Structures

This section presents the conditions for self-equilibrium as well as super-stability of the truncated regular octahedral structure.

5.1 Self-equilibrium conditions

In the symmetry-adapted form, there exists always one zero eigenvalue in $\tilde{\mathbf{E}}_{\mathrm{O}}^{A_1}$ as in Eq. (48). The other three zero eigenvalues come from the three copies of the three-dimensional block $\tilde{\mathbf{E}}_{\mathrm{O}}^{T_1}$, as also indicated in the character table.

Eigenvalues λ of $\tilde{\mathbf{E}}_{\mathrm{O}}^{T_1}$ are calculated by enforcing the following equation to zero:

$$\begin{aligned}
&\det(\tilde{\mathbf{E}}_{\mathrm{O}}^{T_1} - \lambda\mathbf{I}_3) \\
&= \lambda[-\lambda^2 + 4(q_{\mathrm{c}} + q_{\mathrm{e}} + q_{\mathrm{s}})\lambda - 4q_{\mathrm{c}}^2 - 10q_{\mathrm{c}}(q_{\mathrm{e}} + q_{\mathrm{s}}) - 4q_{\mathrm{e}}^2 - 4q_{\mathrm{s}}^2 - 11q_{\mathrm{e}}q_{\mathrm{s}}] \\
&\quad +2[2(q_{\mathrm{e}} + q_{\mathrm{s}})q_{\mathrm{c}}^2 + 2(q_{\mathrm{e}}^2 + q_{\mathrm{s}}^2 + 3q_{\mathrm{e}}q_{\mathrm{s}})q_{\mathrm{c}} + 3q_{\mathrm{e}}q_{\mathrm{s}}(q_{\mathrm{e}} + q_{\mathrm{s}})] \\
&= 0.
\end{aligned} \tag{78}$$

Having zero eigenvalue ($\lambda = 0$) means that

$$\begin{aligned} &2(q_{\rm e}+q_{\rm s})q_{\rm c}^2 + 2(q_{\rm e}^2+q_{\rm s}^2+3q_{\rm e}q_{\rm s})q_{\rm c} + 3q_{\rm e}q_{\rm s}(q_{\rm e}+q_{\rm s}) \\ =&4pq_{\rm e}^2 + (10p^2-2q^2)q_{\rm e} + 6p(p^2-q^2) = 0, \end{aligned} \tag{79}$$

and the other (non-)zero eigenvalues are solved from the following equation:

$$\lambda^2 - 4(q_{\rm c}+q_{\rm e}+q_{\rm s})\lambda + 4q_{\rm c}^2 + 10q_{\rm c}(q_{\rm e}+q_{\rm s}) + 4q_{\rm e}^2 + 4q_{\rm s}^2 - 11q_{\rm e}q_{\rm s} = 0. \tag{80}$$

From Eq. (79), we have the force density $q_{\rm c}$ of cutting cables solved as follows

$$\begin{aligned} q_{\rm c1} &= \frac{q^2-5p^2+\sqrt{p^4+14p^2q^2+q^4}}{4p}, \\ q_{\rm c2} &= \frac{q^2-5p^2-\sqrt{p^4+14p^2q^2+q^4}}{4p}. \end{aligned} \tag{81}$$

Since

$$(q^2-5p^2)^2 - (p^4+14p^2q^2+q^4) = 24p^2(p^2-q^2) < 0, \tag{82}$$

and $\sqrt{p^4+14p^2q^2+q^4} > 0$, we have

$$\begin{aligned} q^2-5p^2+\sqrt{p^4+14p^2q^2+q^4} > 0, \\ q^2-5p^2-\sqrt{p^4+14p^2q^2+q^4} < 0. \end{aligned} \tag{83}$$

In order to ensure $q_{\rm c} > 0$ for carrying tension in cutting cables, we need to consider the following two cases

- For $q_{\rm c1} > 0$, we need

$$p > 0. \tag{84}$$

- For $q_{\rm c2} > 0$, we need

$$p < 0. \tag{85}$$

5.2 Super-stability condition

The one-dimensional block $\tilde{\mathbf{E}}_{\rm O}^{A_2}$ for the octahedral structure is

$$\begin{aligned} \tilde{\mathbf{E}}_{\rm O}^{A_2} &= 4q_{\rm c} + 2q_{\rm e} + 2q_{\rm s} = 4q_{\rm c} + 4p \\ &= \frac{q^2-p^2 \pm \sqrt{p^4+14p^2q^2+q^4}}{p}. \end{aligned} \tag{86}$$

Because

$$(q^2-p^2)^2 - (p^4+14p^2q^2+q^4) = -16q^2p^2 < 0, \tag{87}$$

both solutions for $q_{\rm c} > 0$ with the right p result in positive $\tilde{\mathbf{E}}_{\rm O}^{A_2}$.

From Eq. (80), we can solve the two non-zero eigenvalues for $\tilde{\mathbf{E}}_{\rm O}^{T_1}$ as

$$\lambda_{2,3}^{T_1} = \xi_1 \pm \sqrt{\xi_2} = 2q_{\rm c} + 2q_{\rm e} + 2q_{\rm s} \pm \sqrt{-2q_{\rm c}(q_{\rm e}+q_{\rm s}) - 3q_{\rm e}q_{\rm s}}, \tag{88}$$

where

$$\xi_1 = 2q_c + 2q_e + 2q_s = \frac{q^2 + 3p^2 \pm \sqrt{p^4 + 14p^2q^2 + q^4}}{2p},$$
$$\xi_2 = -2q_c(q_e + q_s) - 3q_eq_s = 2q^2 + 2p^2 \mp \sqrt{p^4 + 14p^2q^2 + q^4}. \tag{89}$$

- For the first solution q_{c1}, we have

$$\xi_1^2 - \xi_2 = \frac{q^4 + 6q^2p^2 + p^4 + (q^2 + 5p^2)\sqrt{p^4 + 14p^2q^2 + q^4}}{2p^2} > 0. \tag{90}$$

  Therefore, the two non-zero eigenvalues $\lambda_{2,3}^{T_1}$ corresponding to q_{c1} are positive.
- For the second solution q_{c2}, we have

$$\xi_1^2 - \xi_2 = \frac{q^4 + 6q^2p^2 + p^4 - (q^2 + 5p^2)\sqrt{p^4 + 14p^2q^2 + q^4}}{2p^2} < 0, \tag{91}$$

  because

$$\begin{aligned} & q^4 + 6q^2p^2 + p^4 - (q^2 + 5p^2)\sqrt{p^4 + 14p^2q^2 + q^4} \\ <& q^4 + 6q^2p^2 + p^4 - (q^2 + 5p^2)(q^2 + p^2) = -4p^2 \\ <& 0. \end{aligned} \tag{92}$$

  Therefore, the smaller one of the two non-zero eigenvalues $\lambda_{2,3}^{T_1}$ corresponding to q_{c1} is negative.

The second solution q_{c2} with $p < 0$ is excluded from further discussions, because there exists one negative eigenvalue in the three-dimensional block $\tilde{\mathbf{E}}_{\mathrm{O}}^{T_1}$, and the corresponding structure cannot be super-stable.

Trace of $\tilde{\mathbf{E}}_{\mathrm{O}}^{E}$ given in Eq. (52) is equal to the sum of its eigenvalues

$$\begin{aligned} \mathrm{tr}(\tilde{\mathbf{E}}_{\mathrm{O}}^{E}) &= \lambda_1^E + \lambda_2^E \\ &= 4q_c + 2q_c + 2q_s = 4q_c + 4p \\ &> 0, \end{aligned} \tag{93}$$

since $p > 0$ for q_{c1}. Moreover, determinant of $\tilde{\mathbf{E}}_{\mathrm{O}}^{E}$ is equal to multiplication of its eigenvalues

$$\begin{aligned} \det(\tilde{\mathbf{E}}_{\mathrm{O}}^{E}) &= \lambda_1^E\lambda_2^E \\ &= 6q_e(q_s + q_c) + 3q_sq_c \\ &= 3(\sqrt{p^4 + 14p^2q^2 + q^4} - 4p^2) \\ &> 3(\sqrt{p^4 + 14p^2p^2 + p^4} - 4p^2) \\ &> 0, \end{aligned} \tag{94}$$

where $q^2 > p^2$ has been applied. Accordingly, the two-dimensional block $\tilde{\mathbf{E}}_{\mathrm{O}}^{E}$ must be positive definite.

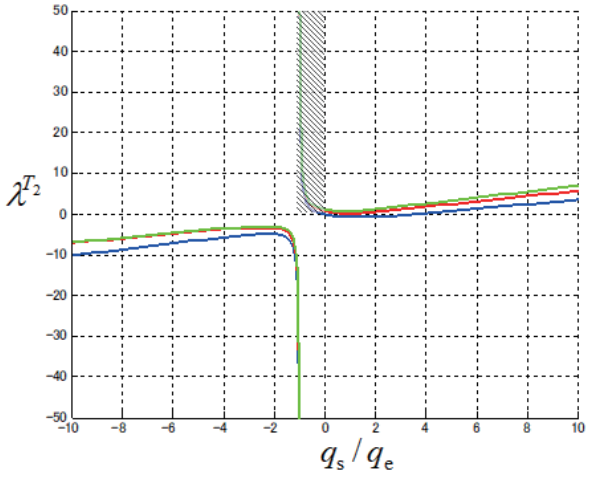

Fig. 7. Eigenvalues λ^{T_2} of $\tilde{\mathbf{E}}_{\mathrm{O}}^{T_2}$ with respect to $q_{\mathrm{s}}/q_{\mathrm{e}}$.

Trace of $\tilde{\mathbf{E}}_{\mathrm{O}}^{T_2}$ given in Eq. (56) is equal to sum of its eigenvalues

$$\begin{aligned}\mathrm{tr}(\tilde{\mathbf{E}}_{\mathrm{O}}^{T_2}) &= \lambda_1^{T_2} + \lambda_2^{T_2} + \lambda_3^{T_2} \\ &= 4q_{\mathrm{c}} + 2q_{\mathrm{c}} + 2q_{\mathrm{s}} = 4q_{\mathrm{c}} + 4p \\ &> 0,\end{aligned} \tag{95}$$

since $p > 0$ for $q_{\mathrm{c}1}$. Moreover, determinant of $\tilde{\mathbf{E}}_{\mathrm{O}}^{T_2}$ is equal to multiplication of its eigenvalues

$$\begin{aligned}\det(\tilde{\mathbf{E}}_{\mathrm{O}}^{T_2}) &= \lambda_1^{T_2}\lambda_2^{T_2}\lambda_3^{T_2} \\ &= 4q_{\mathrm{c}}q_{\mathrm{e}}(q_{\mathrm{e}} + q_2) + 4q_{\mathrm{c}}q_{\mathrm{e}}(q_{\mathrm{e}} + q_{\mathrm{s}}) + 2q_{\mathrm{e}}^2 q_{\mathrm{s}} \\ &= 8q_{\mathrm{c}}p + 2q_{\mathrm{e}}(4q_{\mathrm{c}}p + p^2 - q^2) \\ &> 8q_{\mathrm{c}}p > 0,\end{aligned} \tag{96}$$

since $q_{\mathrm{c}} > 0, p > 0, q_{\mathrm{e}} > 0$, and

$$\begin{aligned}4q_{\mathrm{c}}p + p^2 - q^2 &= -4p^2 + \sqrt{p^4 + 14p^2q^2 + q^4} \\ &> -4p^2 + \sqrt{p^4 + 14p^2p^2 + p^4} = 0.\end{aligned} \tag{97}$$

Accordingly, the eigenvalues of $\tilde{\mathbf{E}}_{\mathrm{O}}^{T_2}$ are highly possible to be positive. Furthermore, its eigenvalues with respect to $q_{\mathrm{s}}/q_{\mathrm{e}}$ are plotted in Fig. 7. It can be observed from the shaded region in Fig. 7 that they are always positive when $-1 < q_{\mathrm{s}}/q_{\mathrm{e}} < 0$; i.e., $p = (q_{\mathrm{e}} - q_{\mathrm{s}})/2 > 0$.

6. Conclusions

In this study, we have presented the conditions for self-equilibrium as well as super-stability for the structures with hexahedral or octahedral symmetry. The conditions are derived in terms of force densities of different types of members. The present analytical method based on group representation theory can be directly applied to any symmetric structures, the nodes of which belong to a single regular orbit; i.e., positions of the nodes

can be exchanged by another node by application of a proper symmetry operation of the group.

The structures with hexahedral or octahedral symmetry consist of only one self-equilibrium prestress mode; although they have two possible solutions, which have been analytically derived by enforcing the symmetry-adapted force density matrix to be singular. The structures with hexahedral or octahedral symmetry have been proved in the study that they are super-stable if and only if the force density of cutting cables is positive and larger than the absolute value of the force density of the struts.

For the truncated regular dodecahedral and icosahedral tensegrity structures, their force density matrices can also be decomposed into smaller blocks by using the same method. However, due to existence of the five-dimensional irreducible representation in the dodecahedral and icosahedral groups, it becomes much difficult to analtically derive the super-stability condition.

Acknowledgment:
The first author gratefully acknowledges the support of JSPS KAKENHI (Grant Number 15KT0109).

REFERENCES

Bishop, Group Theory and Chemistry. Clarendon Press, Oxford, 1973.

Calladine, C.R., 1978. Buckminster Fuller's "tensegrity" structures and Clerk Maxwell's rules for the construction of stiff frames. International Journal of Solids and Structures, 14, 161–172.

Connelly, R. and Back, A., 1998. Mathematics and tensegrity. American Scientist, 86, 142–151.

Connelly, R., 1999. Tensegrity structures: why are they stable? Rigidity Theory and Applications, edited by Thorpe and Duxbury, Kluwer/Plenum Publishers, 47–54.

Fuller, R.B., 1962. Tensile-integrity structures. U.S. Pat. 3,063,521.

Guest S., 2006. The stiffness of prestressed frameworks: A unifying approach, International Journal of Solids and Structures, 43(3-4), pp. 842-854.

Ikeda K., Murota K., 1991. Bifurcation analysis of symmetric structures using block-diagonalization. Comput. Methods Appl. Mech. Engrg., 86, 215–243.

Kangwai, R.D., Guest, S.D. and Pellegrino, S., 1999. Introduction to the analysis of symmetric structures. Computers and Structures, 71(2), 671-688.

Kettle, S.F.A., Symmetry and Structure, 2nd ed. John Wiley & Sons Ltd, West Sussex, England, 1995.

Rimoli, J.J. and Pal, R.K., 2017. Mechanical response of 3-dimensional tensegrity lattices. Composites Part B: Engineering, 115, 30-42.

Rimoli, J.J., 2018. A reduced-order model for the dynamic and post-buckling behavior of tensegrity structures. Mechanics of Materials, 116, 146-157.

Schek, H.-J., 1974. The force density method for form finding and computation of general networks. Computer Methods in Applied Mechanics and Engineering, 3, 115–134.

Thompson, J.M.T., Hunt, G.W., 1984. Elastic Instability Phenomena. John Wiley, Chichester.

Tsuura F., Zhang, J.Y. and Ohsaki, M., 2010. Self-equilibrium and stability of tensegrity structures with polyhedral symmetries. Proceedings of International Association for Shell and Spatial Structures, Shanghai, China, Nov. 2010.

Zhang, J.Y. and Ohsaki, M., 2006. Adaptive force density method for form-finding problem of tensegrity structures. International Journal of Solids and Structures, 43, 5658–5673.

Zhang, J.Y. and Ohsaki, M., 2007. Stability conditions for tensegrity structures. International Journal of Solids and Structures, 44, 3875–3886.

Zhang, J.Y., Guest, S.D. and Ohsaki, M., 2009a. Symmetric prismatic tensegrity structures: part I. configuration and stability. International Journal of Solids and Structures, 46(1), 1–14.

Zhang, J.Y., Guest, S.D. and Ohsaki, M., 2009b. Symmetric prismatic tensegrity structures: part II. symmetry-adapted formulations. International Journal of Solids and Structures, 46(1), 15–30.

Zhang, J.Y., Guest, S.D., Connelly, R. and Ohsaki, M., 2010. Dihedral 'star' tensegrity structures. International Journal of Solids and Structures, 47(1), 1–9.

Zhang, J.Y. and Ohsaki, M., 2012. Self-equilibrium and stability of regular truncated tetrahedral tensegrity structures. Journal of the Mechanics and Physics of Solids, 60(10), 1757–1770, 2012.

Zhang, J.Y. and Ohsaki, M., 2015. Tensegrity Structures: Form, Stability, and Symmetry. Mathematics for Industry 6, Springer, 2015.

Zhang, L.Y., Li, Y., Cao, Y.P., Feng, X.Q., and Gao, H., 2012. Self-equilibrium and super-stability of truncated regular polyhedral tensegrity structures: a unified analytical solution. Proceedings of the Royal Society A: Mathematical, Physical and Engieering

Sciences, 468(2147), 3323–3347.